MULTISCALE MODEL. SIMUL.
Vol. 4, No. 3, pp. 790–812

A MULTISCALE FINITE ELEMENT METHOD FOR NUMERICAL HOMOGENIZATION*

GRÉGOIRE ALLAIRE† AND ROBERT BRIZZI†

Abstract. This paper is concerned with a multiscale finite element method for numerically solving second-order scalar elliptic boundary value problems with highly oscillating coefficients. In the spirit of previous other works, our method is based on the coupling of a coarse global mesh and a fine local mesh, the latter being used for computing independently an adapted finite element basis for the coarse mesh. The main idea is the introduction of a composition rule, or change of variables, for the construction of this finite element basis. In particular, this allows for a simple treatment of high-order finite element methods. We provide optimal error estimates in the case of periodically oscillating coefficients. We illustrate our method in various examples.

Key words. scalar elliptic partial differential equation, multiscale finite element method, numerical homogenization

AMS subject classifications. 35B27, 65N30, 78M40

DOI. 10.1137/040611239

1. Introduction.

The goal of this paper is to build a multiscale finite element for performing numerical homogenization. The word multiscale is understood here in the practical sense that two different meshes will be used: a fine mesh for computing locally and independently (i.e., allowing for an easy parallelization) a finite element basis and a coarse mesh for computing globally and at low cost the solution of an elliptic partial differential equation. By numerical homogenization we mean that we compute not only the mean field solution of a highly heterogeneous problem but also the local fluctuations which may be important in many applications. Recently, there have been many contributions on multiscale numerical methods, including [3], [8], [10], [11], [12], [13], [14], [16], [17]. Our work is in the spirit of that of Hou and Wu [13].

Our model problem is a scalar elliptic partial differential equation which arises in many applications, such as diffusion in porous media or composite materials. Let Ω be a bounded open set of $\mathbb{R}^n$ and $f \in L^2(\Omega)$ (or, more generally, $f \in H^{-1}(\Omega)$). For simplicity, we consider Dirichlet boundary conditions. Our model problem is to find the $u_\varepsilon \in H_0^1(\Omega)$ solution of

$$\left\{ \begin{array}{rcll} -\mathrm{div}\{A^\varepsilon \,\mathrm{grad}\, u^\varepsilon\} & = & f & \text{in } \Omega, \\ \\ u^\varepsilon & = & 0 & \text{on } \partial\Omega, \end{array} \right. \tag{1}$$

where $A^\varepsilon = (a_{ij}^\varepsilon)_{i,j=1}^n$ is a nonnecessarily symmetric matrix of coefficients which all belong to $L^\infty(\Omega)$. We assume that A^ε is uniformly bounded and coercive. The notation $\varepsilon > 0$ stands for some small scale in the problem. (But there could well be several scales, so ε is just a convenient notation for all the small scales of variation of A^ε.) Solving numerically (1) is a difficult task if the scale ε is small. Indeed, a good approximation is obtained with classical finite element methods (or any other

*Received by the editors July 7, 2004; accepted for publication (in revised form) February 23, 2005; published electronically August 22, 2005. This research was supported by the GdR MoMaS CNRS-2439 and sponsored by ANDRA, BRGM, CEA, and EDF.
http://www.siam.org/journals/mms/4-3/61123.html
†CMAP, UMR-CNRS 7641, Ecole Polytechnique, 91128 Palaiseau Cedex, France (gregoire.allaire@polytechnique.fr, robert.brizzi@polytechnique.fr).

methods) only if the mesh size h is smaller than the finest scale, i.e., $h \ll \varepsilon$. As is well known, this is not satisfactory since CPU time as well as memory storage grow polynomially with h^{-1} and soon become prohibitively large.

There is one way out of this difficulty in the special case of periodic heterogeneities or oscillations of the tensor A^ε. In the periodic case, ε is the period, and A^ε is defined by

$$A^\varepsilon(x) = A\left(\frac{x}{\varepsilon}\right),$$

where $y \to A(y)$ is a Y-periodic function in which $Y = (0,1)^n$ is the unit cube. It is a classical result of homogenization theory (see, e.g., [7]) that, for small ε, u^ε is approximated by

$$u^\varepsilon(x) \approx u^*(x) + \varepsilon \sum_{i=1}^{n} \chi_i\left(\frac{x}{\varepsilon}\right) \frac{\partial u^*}{\partial x_i}(x) \tag{2}$$

and

$$\nabla u^\varepsilon(x) \approx \nabla u^*(x) + \sum_{i=1}^{n} (\nabla_y \chi_i)\left(\frac{x}{\varepsilon}\right) \frac{\partial u^*}{\partial x_i}(x), \tag{3}$$

where χ_i is the solution of the so-called cell problem

$$\begin{cases} -\mathrm{div}_y\{A(y)\left(e_i + \mathrm{grad}_y\, \chi_i\right)\} = 0 & \text{in } Y, \\ y \to \chi_i(y) & Y\text{-periodic.} \end{cases} \tag{4}$$

The numerical resolution of (1) is often replaced by the simpler one of the homogenized problem

$$\begin{cases} -\mathrm{div}\{A^* \,\mathrm{grad}\, u^*\} = f & \text{in } \Omega, \\ u^* = 0 & \text{on } \partial\Omega, \end{cases} \tag{5}$$

where A^* is a constant homogenized tensor given by the explicit formula $A^* e_i = \int_Y A(y)\,(e_i + \mathrm{grad}_y\, \chi_i)\, dy$. The approximation of u^ε by u^* can be improved by adding the *first-order corrector term* εu_1. This additional contribution may not be so important in (2) but is crucial in (3) since it is of the same order of magnitude as ∇u^*. Note in passing that (2) and (3) can also be improved by adding a so-called *boundary layer term* since $u^* + \varepsilon u_1$ does not satisfy the Dirichlet boundary condition on $\partial\Omega$ (see, e.g., [4], [5], [6]).

In the nonperiodic case, although there still exist an homogenized problem and approximation formula similar to (2) and (3), the homogenized matrix A^* is unfortunately unknown a priori. Therefore, one cannot replace the numerical resolution of the original problem (1) by that of the homogenized problem (5). Instead, many multiscale numerical methods have been recently devised in order to solve directly (1) but at a price (in terms of CPU time and memory storage) comparable to that of solving (5). Typically, a multiscale finite element method uses a coarse mesh of size $h > \varepsilon$ and an adapted finite element basis which incorporates the small-scale features of the oscillating tensor A^ε. The finite element basis is precomputed locally on each cell of the coarse mesh (and in parallel for computational efficiency) by solving a local

version of (1). The number of degrees of freedom is thus not larger than for a classical finite element method on the coarse mesh.

Let us describe the main idea behind our new multiscale finite element method. Although it is designed for nonperiodic homogenization problems, for the sake of simplicity we first present it in the context of periodic homogenization. A key idea is to remark that (2) looks like a first-order Taylor expansion; namely, it implies

$$u^\varepsilon(x) \approx u^*\left(x + \varepsilon\chi\left(\frac{x}{\varepsilon}\right)\right), \tag{6}$$

where $\chi = (\chi_1, \ldots, \chi_n)$. The approximation formula (6) was already used by Kozlov [15] for the homogenization of random operators. Building on (6), we introduce a coarse mesh of size $h > \varepsilon$ and a classical conforming finite element basis $(\Phi_l^h)_l$, and we define an *oscillating finite element basis* through the same composition rule:

$$\Phi_l^{\varepsilon,h}(x) = \Phi_l^h\left(x + \varepsilon\chi\left(\frac{x}{\varepsilon}\right)\right).$$

Our method amounts to applying a standard Galerkin procedure to the variational formulation of (1) with this oscillating finite element basis. The advantages of our method are at least twofold. First, it is very easy to implement high-order methods since the computation of the oscillating functions $\chi(\frac{x}{\varepsilon})$ is independent of the order of the coarse mesh finite element basis $(\Phi_l^h)_l$. Second, the convergence analysis is somehow simpler since, roughly speaking, it amounts to applying the change of variables $x \to x + \varepsilon\chi(\frac{x}{\varepsilon})$ to a standard convergence result on the coarse mesh. However, one drawback of our method is that it applies only to scalar second-order elliptic partial differential equations. We do not know if an approximation formula similar to (6) holds for systems of equations such as, for example, the linearized elasticity system.

The content of the paper is as follows. In section 2, we recall some basic facts of homogenization theory and give a precise statement about (6) in the general (nonperiodic) case. Section 3 is devoted to a precise definition of our multiscale finite element method. Its convergence is then studied in section 4. Finally, in section 5 some numerical results are given.

2. Some results in homogenization theory.

2.1. H-convergence and oscillating test functions. Let us recall some results of the H-convergence theory (for details see, e.g., [19], [2]). Let $\mathcal{M}_n$ be the linear space of square real matrices of order n, and define, for given positive constants $\alpha > 0$ and $\beta > 0$, the subspace of $\mathcal{M}_n$ made up of matrices which are coercive as well as their inverses:

$$\mathcal{M}_{\alpha,\beta} = \left\{M \in \mathcal{M}_n\,;\, M\xi.\xi \geq \alpha|\xi|^2\,,\, M^{-1}\xi.\xi \geq \beta|\xi|^2 \quad \forall \xi \in \mathbb{R}^n\right\}.$$

A sequence of matrices $A^\varepsilon \in L^\infty(\Omega; \mathcal{M}_{\alpha,\beta})$ is said to H-converge, when ε tends to zero, to a homogenized matrix $A^* \in L^\infty(\Omega; \mathcal{M}_{\alpha,\beta})$ if, for any right-hand side $f \in H^{-1}(\Omega)$, the sequence of solutions u^ε of (1) satisfies

$$\begin{aligned} u^\varepsilon &\rightharpoonup u^* \text{ weakly in } H_0^1(\Omega) \quad (\varepsilon \to 0), \\ A^\varepsilon \operatorname{grad} u^\varepsilon &\rightharpoonup A^* \operatorname{grad} u^* \text{ weakly in } L^2(\Omega)^n \quad (\varepsilon \to 0), \end{aligned}$$

where u^* denotes the solution of the homogenized equation (5). This definition makes sense because of the following sequential compactness property [19].

THEOREM 2.1. *Let $(A^\varepsilon)_{\varepsilon>0}$ be a sequence of matrices in $L^\infty(\Omega;\mathcal{M}_{\alpha,\beta})$. There exists a subsequence, still denoted by ε, and a homogenized matrix $A^* \in L^\infty(\Omega;\mathcal{M}_{\alpha,\beta})$ such that A^ε H-converges to A^*.*

Except in the periodic case, this abstract result does not give an explicit formula for the limit A^*. Actually, the homogenized tensor A^* is defined as a limit in the distributional sense, namely

$$A^\varepsilon(x)\,\mathrm{grad}\,\widehat{w}_i^\varepsilon \;\rightharpoonup\; A^* e_i \text{ in } \mathscr{D}'(\Omega;\mathbb{R}^n),$$

where $(e_i)_{i=1,n}$ denotes the canonical basis of $\mathbb{R}^n$, and $(\widehat{w}_i^\varepsilon)_{i=1,n}$ are the so-called *oscillating test functions* which satisfy

$$\widehat{w}_i^\varepsilon \;\rightharpoonup\; x_i \text{ weakly in } H^1(\Omega), \tag{7}$$

and

$$g_i^\varepsilon \;=\; -\mathrm{div}\{A^\varepsilon \mathrm{grad}\,\widehat{w}_i^\varepsilon\} \;\longrightarrow\; g_i \;=\; -\mathrm{div}\{A^* e_i\} \text{ strongly in } H^{-1}(\Omega) \tag{8}$$

when $\varepsilon \to 0$. The existence of such oscillating test functions is the key point in the proof of Theorem 2.1, but they are neither explicit (since they depend on A^*) nor unique (since they are unique up to the addition of a sequence converging strongly to zero in $H^1(\Omega)$). For our purpose, we define them as the solutions of the following boundary value problems ($j = 1, \ldots, n$):

$$\left\{\begin{array}{rcll} -\mathrm{div}\{A^\varepsilon\,\mathrm{grad}\,\widehat{w}_j^\varepsilon\} & = & -\mathrm{div}\{A^*\,e_j\} & \text{in } \Omega, \\ \widehat{w}_j^\varepsilon & = & x_j & \text{on } \partial\Omega. \end{array}\right. \tag{9}$$

These oscillating test functions are also useful for obtaining a corrector result.

THEOREM 2.2. *Let $(A^\varepsilon)_{\varepsilon>0}$ be a sequence H-converging to A^* in $L^\infty(\Omega;\mathcal{M}_{\alpha,\beta})$. Then*

$$\mathrm{grad}\,u^\varepsilon \;=\; \sum_{i=1}^n \nabla\widehat{w}_i^\varepsilon \frac{\partial u^*}{\partial x_i} \;+\; r_\varepsilon, \tag{10}$$

where the remainder r_ε converges strongly to zero in $L^1(\Omega;\mathbb{R}^n)$. Furthermore, if $u^* \in W^{1,\infty}(\Omega)$, then r_ε converges strongly in $L^2(\Omega;\mathbb{R}^n)$.

Remark 2.3. In the context of Theorem 2.2 it is clear that, if the homogenized solution is smoother, say $u^* \in W^{2,\infty}(\Omega)$, then

$$u^\varepsilon = u^* + \sum_{i=1}^n (\widehat{w}_i^\varepsilon(x) - x_i)\,\frac{\partial u^*}{\partial x_i} \;+\; r'_\varepsilon, \tag{11}$$

where the remainder r'_ε converges strongly to zero in $H^1(\Omega)$. In what follows, we denote by

$$[\widehat{W}^\varepsilon] \;=\; \left[\left(\frac{\partial\widehat{w}_j^\varepsilon}{\partial x_i}\right)_{i,j=1,n}\right] \tag{12}$$

the so-called corrector matrix.

Proof. The proof of (10) is classical (see, e.g., [2]). The last statement of Theorem 2.2 is simpler to prove, so we briefly explain how to proceed. Using the coercivity of A^ε we are done if we can show that

$$\lim_{\varepsilon\to 0}\int_\Omega A^\varepsilon\left(\operatorname{grad} u^\varepsilon - [\widehat{W}^\varepsilon]\operatorname{grad} u^*\right)\cdot\left(\operatorname{grad} u^\varepsilon - [\widehat{W}^\varepsilon]\operatorname{grad} u^*\right)\,dx = 0. \tag{13}$$

Developing the scalar product in the integral (13), we obtain the following terms:

$$\int_\Omega [\widehat{W}^\varepsilon]^t A^\varepsilon [\widehat{W}^\varepsilon]\operatorname{grad} u^*\cdot\operatorname{grad} u^*\,dx + \int_\Omega A^\varepsilon \operatorname{grad} u^\varepsilon\cdot\operatorname{grad} u^\varepsilon\,dx$$

$$- \int_\Omega A^\varepsilon \operatorname{grad} u^\varepsilon\cdot[\widehat{W}^\varepsilon]\operatorname{grad} u^*\,dx - \int_\Omega A^\varepsilon\,[\widehat{W}^\varepsilon]\operatorname{grad} u^*\cdot\operatorname{grad} u^\varepsilon\,dx.$$

To pass to the limit in the first term we use the facts (see Lemma 1.3.38 in [2]) that $[\widehat{W}^\varepsilon]^t A^\varepsilon[\widehat{W}^\varepsilon]$ converges to A^* in $\mathscr{D}'(\Omega;\mathscr{M}_n)$ and that, thanks to Meyers' theorem [18], which implies a uniform $L^p(\Omega)$ bound (with $p>2$) for $[\widehat{W}^\varepsilon]$, this convergence holds true weakly in $L^1(\Omega;\mathscr{M}_n)$. Thus, since $u^*\in W^{1,\infty}(\Omega)$, we have

$$\int_\Omega [\widehat{W}^\varepsilon]^t A^\varepsilon[\widehat{W}^\varepsilon]\operatorname{grad} u^*\cdot\operatorname{grad} u^*\,dx \longrightarrow \int_\Omega A^*\operatorname{grad} u^*\cdot\operatorname{grad} u^*\,dx.$$

The second term is easy:

$$\int_\Omega A^\varepsilon\operatorname{grad} u^\varepsilon\cdot\operatorname{grad} u^\varepsilon\,dx = \int_\Omega f\,u^\varepsilon\,dx \longrightarrow \int_\Omega f\,u^*\,dx = \int_\Omega A^*\operatorname{grad} u^*\cdot\operatorname{grad} u^*\,dx.$$

Applying the "div-curl" compensated compactness result [19] to the third term and using the regularity assumptions as well as Meyers' theorem, we get the desired result:

$$\int_\Omega A^\varepsilon\operatorname{grad} u^\varepsilon\cdot[\widehat{W}^\varepsilon]\operatorname{grad} u^*\,dx \longrightarrow \int_\Omega A^*\operatorname{grad} u^*\cdot\operatorname{grad} u^*\,dx.$$

The fourth term is treated in the same way, and their combination gives zero. ∎

2.2. A remark on the corrector result. The right-hand side of formula (11) looks like the first-order Taylor expansion of u^* at the point $\widehat{w}^\varepsilon(x)=(\widehat{w}_1^\varepsilon(x),\dots,\widehat{w}_n^\varepsilon(x))$. It indicates that $u^\varepsilon(x)$ may well be approximated by $u^*\circ\widehat{w}^\varepsilon(x)$. This remark has already been made by Kozlov [15] in a different context, namely the homogenization of random operators. This change of variables was called by Kozlov "harmonic coordinates." It yields the following new formulation of the corrector result given by Theorem 2.2.

THEOREM 2.4. *Let $(A^\varepsilon)_{\varepsilon>0}$ be a sequence H-converging to A^* in $L^\infty(\Omega;\mathcal{M}_{\alpha,\beta})$. For $f\in H^{-1}(\Omega)$, let u^ε be the solution of* (1) *and u^* be that of* (5). *Let $\widehat{w}_j^\varepsilon$ be the family of oscillating test functions defined in* (9). *Assume that $u^*\in W^{2,\infty}(\Omega)$. Then*

$$u^\varepsilon = u^*\circ\widehat{w}^\varepsilon + \widehat{r}^\varepsilon, \tag{14}$$

where the remainder term $\widehat{r}^\varepsilon$ converges strongly to zero in $H_0^1(\Omega)$.

Remark 2.5. The approximation of the *principal part of the solution* u^ε, i.e., $u^*\circ\widehat{w}^\varepsilon$, may serve as a substitute for the approximation of the solution of problem (1). This idea is at the root of the new multiscale finite element method described in this work.

Proof. It is not clear that $\widehat{w}^\varepsilon(\Omega) \subset \Omega$ (see Lemma 2.9), so formula (14) makes sense if u^* is first extended by zero outside Ω. Since u^* is a Lipschitz function, $u^* \circ \widehat{w}^\varepsilon$ belongs to $H^1(\Omega)$. Furthermore, since $\widehat{w}^\varepsilon(x) = x$ a.e. on $\partial\Omega$, the function $u^* \circ \widehat{w}^\varepsilon$ belongs to $H_0^1(\Omega)$. We have

$$\|u^\varepsilon - u^* \circ \widehat{w}^\varepsilon\|_{H_0^1(\Omega)} = \|\operatorname{grad} u^\varepsilon - \operatorname{grad}(u^* \circ \widehat{w}^\varepsilon)\|_{L^2(\Omega)^n} \tag{15}$$

$$\leq \|\operatorname{grad} u^\varepsilon - [\widehat{W}^\varepsilon] \operatorname{grad} u^*\|_{L^2(\Omega)^n} + \|[\widehat{W}^\varepsilon] (\operatorname{grad} u^* - (\operatorname{grad} u^*) \circ \widehat{w}^\varepsilon)\|_{L^2(\Omega)^n}.$$

The first term in the right-hand side of (15) tends to zero because of Theorem 2.2. The second term is bounded by

$$\|[\widehat{W}^\varepsilon] (\operatorname{grad} u^* - (\operatorname{grad} u^*) \circ \widehat{w}^\varepsilon)\|_{L^2(\Omega)^n}$$

$$\leq \|[\widehat{W}^\varepsilon]\|_{L^p(\Omega;\mathcal{M}_n)} \|\operatorname{grad} u^* - (\operatorname{grad} u^*) \circ \widehat{w}^\varepsilon\|_{L^{p'}(\Omega)^n}$$

with $1/p + 1/p' = 1/2$. A Taylor expansion with integral remainder yields

$$(\operatorname{grad} u^*) \circ \widehat{w}^\varepsilon = \operatorname{grad} u^* + \int_0^1 \nabla\nabla\, u^*(x + t(\widehat{w}^\varepsilon(x) - x)).(\widehat{w}^\varepsilon(x) - x)\, dt,$$

and thus we obtain

$$\|(\operatorname{grad} u^*) \circ \widehat{w}^\varepsilon - \operatorname{grad} u^*\|_{L^{p'}(\Omega)^n} \leq \|u^*\|_{W^{2,\infty}(\Omega)} \|\widehat{w}^\varepsilon - x\|_{L^{p'}(\Omega;\mathbb{R}^n)^n}.$$

By Meyers' theorem there exists $p > 2$ such that $\|[\widehat{W}^\varepsilon]\|_{L^p(\Omega;\mathcal{M}_n)}$ is uniformly bounded. By the weak maximum principle (see Theorem 4.1 in [21]), $(\widehat{w}^\varepsilon - x)$ is uniformly bounded in $L^\infty(\Omega;\mathbb{R}^n)^n$, and since it converges strongly to zero in $L^2(\Omega;\mathbb{R}^n)^n$, it also converges strongly in $L^{p'}(\Omega;\mathbb{R}^n)^n$. Altogether this implies that the second term in the right-hand side of (15) tends to zero. ∎

There is a converse statement of Theorem 2.4.

THEOREM 2.6. *Let $(A^\varepsilon)_{\varepsilon>0}$ be a sequence H-converging to A^* in $L^\infty(\Omega;\mathcal{M}_{\alpha,\beta})$. For $f \in H^{-1}(\Omega)$, let u^ε be the solution of (1) and $\widehat{w}^\varepsilon$ be the family of oscillating test functions defined in (9). If there exists a function $u \in H_0^1(\Omega) \cap W^{1,\infty}(\Omega)$ such that*

$$\|u^\varepsilon - u \circ \widehat{w}^\varepsilon\|_{H_0^1(\Omega)} \longrightarrow 0 \text{ when } \varepsilon \to 0,$$

then $u = u^*$, the solution of the homogenized problem (5).

Proof. By assumption, u^ε admits the following representation formula, similar to (14):

$$u^\varepsilon = u \circ \widehat{w}^\varepsilon + \tilde{r}^\varepsilon, \tag{16}$$

where $\tilde{r}^\varepsilon$ converges strongly to zero in $H_0^1(\Omega)$. Let us consider the variational formulation of (1):

$$a^\varepsilon(u^\varepsilon, v) = \int_\Omega A^\varepsilon \operatorname{grad} u^\varepsilon \cdot \operatorname{grad} v\, dx = \int_\Omega f\, v\, dx \quad \forall v \in H_0^1(\Omega). \tag{17}$$

Substituting (16) into (17) gives

$$\int_\Omega A^\varepsilon [\widehat{W}^\varepsilon] (\operatorname{grad} u) \circ \widehat{w}^\varepsilon \cdot \operatorname{grad} v\, dx + \int_\Omega A^\varepsilon \operatorname{grad} \tilde{r}^\varepsilon \cdot \operatorname{grad} v\, dx = \int_\Omega f\, v\, dx \quad \forall v \in H_0^1(\Omega).$$

By assumption the second integral tends to zero, while the first one converges to $\int_\Omega A^*\nabla u \cdot \nabla v\, dx$. Indeed, by H-convergence, $A^\varepsilon[\widehat{W}^\varepsilon]$ converges weakly to A^* in $L^2(\Omega;\mathscr{M}_n)$, and, by the Lebesgue dominated convergence theorem, $(\operatorname{grad} u)\circ\widehat{w}^\varepsilon$ converges strongly to $\operatorname{grad} u$ in $L^2(\Omega)^n$. Thus, passing to the limit we obtain that u is a solution of the variational formulation of the homogenized problem (5), i.e., $u = u^*$. ∎

2.3. An approximate variational formulation. The representation formula (14) for u_ε suggests an approximation of the variational formulation (17). Indeed, it is equivalent to

$$a^\varepsilon(\, u^*\circ\widehat{w}^\varepsilon\,,\, v\,) \;=\; \int_\Omega f\, v\, dx \;-\; a^\varepsilon(\,\widehat{r}^\varepsilon\,,\, v\,) \quad \forall v\in H^1_0(\Omega), \tag{18}$$

where the last term tends to zero. Dropping it and choosing an adequate subspace of $H^1_0(\Omega)$ should yield a good approximation of (17). A first possible choice of subspace is

$$\big\{v^\varepsilon \in H^1_0(\Omega)\,;\, \exists\, v\in H^1_0(\Omega)\cap W^{1,\infty}(\Omega)\,,\; v^\varepsilon \;=\; v\circ\widehat{w}^\varepsilon\big\},$$

but it is unfortunately not closed in $H^1_0(\Omega)$, so it cannot be a Hilbert space. Another possibility, which requires the additional regularity $\widehat{w}^\varepsilon\in W^{1,\infty}(\Omega;\mathbb{R}^n)$, is

$$V^\varepsilon \;=\; \big\{v^\varepsilon \in H^1_0(\Omega)\,;\, \exists\, v\in H^1_0(\Omega)\,,\; v^\varepsilon \;=\; v\circ\widehat{w}^\varepsilon\big\}, \tag{19}$$

which is a closed subspace of $H^1_0(\Omega)$ since $\widehat{w}^\varepsilon\in W^{1,\infty}(\Omega;\mathbb{R}^n)$ implies that $v\circ\widehat{w}^\varepsilon$ belongs to $H^1_0(\Omega)$ as soon as v does. We defined the approximate variational formulation as follows: find $u\in H^1_0(\Omega)$ such that

$$a^\varepsilon(u\circ\widehat{w}^\varepsilon, v\circ\widehat{w}^\varepsilon) \;=\; \int_\Omega f v\circ\widehat{w}^\varepsilon dx \quad \forall v\in H^1_0(\Omega). \tag{20}$$

By the Lax–Milgram theorem, (20) admits a unique solution $u\circ\widehat{w}^\varepsilon$ in V^ε. In the following, we will call u the *substituting homogenized solution*. Remark that u actually depends on ε, but it oscillates less compared to u_ε.

LEMMA 2.7. *Assume $\widehat{w}^\varepsilon\in W^{1,\infty}(\Omega;\mathbb{R}^n)$. Let u be the unique solution of* (20) *and u^* be the solution of the homogenized problem* (5). *Then*

$$\|(u-u^*)\circ\widehat{w}^\varepsilon\|_{H^1_0(\Omega)} \;\to\; 0 \quad \textit{when } \varepsilon\to 0.$$

Remark 2.8. Of course, combining Lemma 2.7 and our corrector result, Theorem 2.4, we deduce that $u\circ\widehat{w}^\varepsilon$ is a good approximation of the solution u_ε of the original problem (1):

$$\|u^\varepsilon - u\circ\widehat{w}^\varepsilon\|_{H^1_0(\Omega)} \;\to\; 0 \quad \text{when } \varepsilon\to 0.$$

Proof. Subtracting (20) from (18) with the same test function $(v\circ\widehat{w}^\varepsilon)\in V^\varepsilon\subset H^1_0(\Omega)$ we obtain

$$a^\varepsilon(\,(u-u^*)\circ\widehat{w}^\varepsilon\,,\, v\circ\widehat{w}^\varepsilon\,) \;=\; a^\varepsilon(\,\widehat{r}^\varepsilon\,,\, v\circ\widehat{w}^\varepsilon\,).$$

Taking $v = u-u^*$ and using the coercivity and continuity of the bilinear form show that

$$\alpha\,\|(u-u^*)\circ\widehat{w}^\varepsilon\|_{H^1_0(\Omega)} \;\le\; \beta^{-1}\;\|\widehat{r}^\varepsilon\|_{H^1_0(\Omega)},$$

which tends to zero as ε does. ∎

2.4. Change of variables. A reasonable question to ask is whether the mapping $x \to w^\varepsilon(x)$ from Ω into $\mathbb{R}^n$ is a change of variables, i.e., is one-to-one into Ω. We do not know if it is true in general. Nevertheless, we have the following partial results.

LEMMA 2.9. *Assume $\widehat{w}^\varepsilon \in W^{1,\infty}(\Omega)^n$. Then the mapping $\widehat{w}^\varepsilon$ is onto in the sense that $\widehat{w}^\varepsilon(\overline{\Omega}) \supset \overline{\Omega}$.*

Proof. Since $\widehat{w}^\varepsilon = x$ on $\partial\Omega$ and $W^{1,\infty}(\Omega) \subset C^0(\overline{\Omega})$, then, from topological degree theory [20],

$$deg(\widehat{w}^\varepsilon, \Omega, y) \;=\; deg(id, \Omega, y) \;\forall y \notin \partial\Omega,$$

where id denotes the canonical injection from Ω into $\mathbb{R}^n$. On the other hand,

$$deg(id, \Omega, y) \;=\; \begin{cases} 1 & \text{if} \quad y \in \Omega, \\ \\ 0 & \text{if} \quad y \notin \Omega. \end{cases}$$

Thus, for $y \in \Omega$, $deg(\widehat{w}^\varepsilon, \Omega, y) \neq 0$ and from topological degree property, we deduce that there exists an $x \in \Omega$ such that $y = \widehat{w}^\varepsilon(x)$. ∎

The question of injectivity is much more delicate. Let us simply recall the following result of [1].

THEOREM 2.10. *Assume $\Omega \subset \mathbb{R}^2$ is a bounded simply connected open set whose boundary $\partial\Omega$ is a convex closed curve. Assume further that $A^\varepsilon(x)$ is symmetric and that A^* does not depend on x. Then the mapping $\widehat{w}^\varepsilon$ is a homeomorphism from $\overline{\Omega}$ into itself.*

Remark 2.11. The homogenized matrix A^* is constant, for example, in the case of periodic homogenization, i.e., $A^\varepsilon(x) = A(\frac{x}{\varepsilon})$.

Remark 2.12. In the case of small amplitude homogenization, one can prove that the mapping $\widehat{w}^\varepsilon$ is a homeomorphism. Indeed, by a perturbation argument, if $A^\varepsilon(x)$ is close to a constant matrix A_0, then $\widehat{w}^\varepsilon(x)$ is close to x and thus is one-to-one. To be more precise, we should choose adequate norms for measuring the closedness. For example, one may take the $C^{1,\alpha}$-norm for the matrices $A^\varepsilon(x)$ and A_0 and the $C^{2,\alpha}$-norm for the solutions $\widehat{w}^\varepsilon(x)$ and x.

2.5. Technical lemmas. We now state two technical lemmas which are used in the proof of the convergence theorem (Theorem 4.1) studied in section 4. We first recall a classical corrector result in periodic homogenization [7], where the dependence on the size of the domain is made explicit. (For a proof, see [13].) Let ω be a smooth bounded open set, $f \in L^2(\omega)$, and $g \in H^1(\omega)$. Define the original problem

$$\begin{cases} -\text{div}\{A^\varepsilon \text{ grad } v^\varepsilon\} &= f \quad \text{in } \omega, \\ v^\varepsilon &= g \quad \text{on } \partial\omega \end{cases}$$

and its homogenized limit

$$\begin{cases} -\text{div}\{A^* \text{ grad } v^*\} &= f \quad \text{in } \omega, \\ v^* &= g \quad \text{on } \partial\omega. \end{cases}$$

LEMMA 2.13. *There exists a constant C, which is independent of ε, ω, and the data f, g, such that*

$$\left\| v^\varepsilon \;-\; v^* \;-\; \varepsilon \sum_{i=1}^{n} \chi_i \left(\frac{x}{\varepsilon}\right) \frac{\partial v^*}{\partial x_i}(x) \right\|_{H^1(\omega)} \;\leq\; C\sqrt{\varepsilon}\, \sqrt{|\partial\omega|}\, \|v^*\|_{W^{2,\infty}(\omega)}.$$

The second lemma is a quantitative version of Theorem 2.4 in the periodic case. Remark, however, that it involves the solution of the cell problem instead of the oscillating test function $\widehat{w}^\varepsilon$ defined by (9).

LEMMA 2.14. *Let $\widetilde{w}^\varepsilon$ be defined by* (32). *Assume that $u^* \in W^{2,\infty}(\Omega)$ and $\chi_i \in W^{1,\infty}(Y)$. Then there exists a constant C, independent of ε, such that*

$$\|u^\varepsilon - u^* \circ \widetilde{w}^\varepsilon\|_{H^1_0(\Omega)} \leq C\sqrt{\varepsilon}.$$

Proof. We have

$$\begin{aligned} \|\nabla u^\varepsilon - \nabla (u^* \circ \widetilde{w}^\varepsilon)\|_{L^2(\Omega)^n} &\leq \|\nabla u^\varepsilon - [\nabla \widetilde{w}^\varepsilon]\, \nabla u^*\|_{L^2(\Omega)^n} \\ &+ \|[\nabla \widetilde{w}^\varepsilon]\, (\nabla u^* - (\nabla u^*) \circ \widetilde{w}^\varepsilon)\|_{L^2(\Omega)^n}. \end{aligned} \tag{21}$$

Since $[\nabla \widetilde{w}^\varepsilon(x)] = Id + [\nabla_y \chi]\,(\frac{x}{\varepsilon})$, the first term in the right-hand side of (21) is bounded by $\sqrt{\varepsilon}$ by a classical corrector result (see Lemma 2.13). The second term is bounded by

$$\|Id + [\nabla_y \chi]\|_{L^\infty(Y)}\ \|\nabla u^* - (\nabla u^*) \circ \widetilde{w}^\varepsilon\|_{L^2(\Omega)^n}.$$

A Taylor expansion with integral remainder yields

$$(\nabla u^*) \circ \widetilde{w}^\varepsilon = \nabla u^* + \varepsilon \int_0^1 \nabla\nabla u^* \left(x + \varepsilon t \chi\left(\frac{x}{\varepsilon}\right)\right) \cdot \chi\left(\frac{x}{\varepsilon}\right) dt,$$

and thus we obtain

$$\|(\nabla u^*) \circ \widetilde{w}^\varepsilon - \nabla u^*\|_{L^2(\Omega)^n} \leq \varepsilon \|u^*\|_{W^{2,\infty}(\Omega)} \| \chi \|_{L^2(\Omega)^n},$$

which gives the desired result. ∎

3. Definition of the multiscale finite element method.

3.1. Approximation of the oscillating test functions. The idea of our multiscale finite element method is to solve the approximate variational formulation (20) instead of the true one (17). This requires the computation of the oscillating test functions which are not explicit since, in view of their definition (9), they depend on A^*, which is unknown. Therefore, we need to introduce an adequate approximation procedure.

We introduce a coarse mesh of Ω which, for simplicity, is assumed to be polyhedral. This coarse mesh is a conforming triangulation $\mathcal{T}_h$ such that

$$\overline{\Omega} = \bigcup_{K \in \mathcal{T}_h} K, \tag{22}$$

where the elements K satisfy $\mathrm{diam}(K) \leq h$. In practice the mesh size h is larger than the space scale of oscillations ε, i.e., $h > \varepsilon$. For each $K \in \mathcal{T}_h$, let us define $\widehat{w}_i^{\varepsilon,K}$ $(i = 1, \ldots, n)$ as the solution of

$$\begin{cases} -\mathrm{div}\{A^\varepsilon\, \mathrm{grad}\, \widehat{w}_i^{\varepsilon,K}\} = -\mathrm{div}\{A_K^*\, \mathrm{grad}\, x_i\} & \text{in } K, \\ \widehat{w}_i^{\varepsilon,K} = x_i & \text{on } \partial K, \end{cases} \tag{23}$$

where A_K^* is a local approximation of A^* in K. The simplest approximation is to take A_K^* constant in K: in such a case its precise value is irrelevant since the right-hand

side of (23) cancels out. This will be our choice in the numerical examples of this paper. Nevertheless, it is possible to take $A^*_K(x)$ as some varying local average of A^ε.

Collecting these local approximations we define $\widehat{w}_i^{\varepsilon,h} \in H^1(\Omega)$ by $\widehat{w}_i^{\varepsilon,h} = \widehat{w}_i^{\varepsilon,K}$ for each $K \in \mathcal{T}_h$, and we set $\widehat{w}^{\varepsilon,h} = (\widehat{w}_1^{\varepsilon,h}, \dots, \widehat{w}_n^{\varepsilon,h}) \in H^1(\Omega; \mathbb{R}^n)$.

A numerical approximation of the local oscillating test functions defined in (23) is computed by using a classical conforming finite element in each $K \in \mathcal{T}_h$. For each coarse mesh cell K we introduce a local fine mesh $\mathcal{T}_{h'}^K$, where h' denotes the size of this fine mesh. Of course, we have $h' < h$, but, since we want to resolve the oscillations of the tensor A^ε, we also have $h' < \varepsilon$. We consider $\mathbb{P}_{k'}$ Lagrange finite elements for solving the local boundary value problems (23). Since, from one cell K to the other, these problems are independent, this may be done in parallel. This procedure is very similar to that introduced in [13].

The *hats* used in our notation refer to exact solutions of boundary value problems: thus $\widehat{w}^\varepsilon$ refers to the "true" oscillating test function, and $\widehat{w}^{\varepsilon,h}$ refers to the collection over $\mathcal{T}_h$ of all solutions of (23). We shall drop the *hat notation* when we refer to the corresponding numerical approximations: thus $w_i^{\varepsilon,K}$ is the $\mathbb{P}_{k'}$ finite element approximation of $\widehat{w}_i^{\varepsilon,K}$, and $w_i^{\varepsilon,h}$, $w^{\varepsilon,h}$ are defined as above with the hat notation. In numerical practice we content ourselves in using $\mathbb{P}_1$ finite elements for computing $w^{\varepsilon,h}$.

3.2. A multiscale finite element method. Let $V_h \subset H_0^1(\Omega)$ be a finite dimensional subspace ($\dim V_h = N_h$) corresponding to a conforming finite element method defined on the coarse mesh (23). Typically, we use $\mathbb{P}_k$ Lagrange finite elements. Let $(\Phi_l^h)_{l=1,\dots,N_h}$ denote a finite element basis of V_h. In order to compute a numerical approximation u_h of the substituting homogenized solution u, we introduce an *oscillating (or multiscale) finite element basis* defined by

$$\Phi_l^{\varepsilon,h}(x) \;=\; \Phi_l^h \circ w^{\varepsilon,h}(x) \quad (l = 1, \dots, N_h). \tag{24}$$

We therefore obtain a conformal finite element method associated with the coarse mesh $\mathcal{T}_h$, and we denote by $V_h^\varepsilon \subset H_0^1(\Omega)$ the space spanned by the functions $(\Phi_l^{\varepsilon,h})_{l=1,\dots,N_h}$. Roughly speaking, V_h^ε is the space "$V_h \circ w^{\varepsilon,h}$."

From the approximate variational formulation (20), we deduce a numerical approximation: find $u_h \circ w^{\varepsilon,h} \in V_h^\varepsilon$ such that

$$a^\varepsilon(u_h \circ w^{\varepsilon,h}, v_h \circ w^{\varepsilon,h}) \;=\; \int_\Omega f\, v_h \circ w^{\varepsilon,h}\, dx \quad \forall v_h \circ w^{\varepsilon,h} \in V_h^\varepsilon. \tag{25}$$

We use Lagrange finite elements, and, consequently, the degrees of freedom are the values at the nodes n_j^K $(j = 1, \dots, N_K)$ of the elements $K \in \mathcal{T}_h$. For such an element K, let $\Phi^{\varepsilon,K}$ be the associated local basis which is made up of N_K polynomials $p_i^K \in \mathbb{P}_k$ satisfying $p_i^K(n_j^K) = \delta_{ij}$. The local oscillating finite element basis is

$$\Phi_i^{\varepsilon,K}(x) \;=\; p_i^K \circ w^{\varepsilon,K}(x), \tag{26}$$

and, since $w^{\varepsilon,K}(x) = x$ on ∂K, it still satisfies on the boundary nodes

$$\Phi_i^{\varepsilon,K}(n_j^K) \;=\; \delta_{ij} \quad \forall n_j^K \in \partial K.$$

On the other hand, for each $K \in \mathcal{T}_h$,

$$(u_h \circ w^{\varepsilon,K})|_K(x) \;=\; [\Phi^{\varepsilon,K}(x)]\, \{u_h^K\},$$

where $[\Phi^{\varepsilon,K}(x)] = [\Phi_1^{\varepsilon,K}, \ldots, \Phi_{N_K}^{\varepsilon,K}]$ and $\{u_h^K\}$ is the column vector composed of values of u_h at the nodes of K.

Remark 3.1. In the case of piecewise linear finite elements $\mathbb{P}_1$ we recover the multiscale finite element method previously introduced by Hou and Wu [13]. Indeed, when the basis functions p_i^K belong to $\mathbb{P}_1$, by linearity the oscillating basis functions can be written

$$\Phi_i^{\varepsilon,K}(x) \;=\; p_i^K(x) \;+\; \sum_{j=1}^{n} \Big(w_j^{\varepsilon,K}(x) - x_j \Big) \frac{\partial p_i^K}{\partial x_j}(x). \tag{27}$$

A simple calculation shows that

$$\operatorname{div}\{A^\varepsilon \operatorname{grad} \Phi_i^{\varepsilon,K}\} \;=\; \sum_{j=1}^{n} \operatorname{div}\{A^\varepsilon \operatorname{grad} w_j^{\varepsilon,K}\} \frac{\partial p_i^K}{\partial x_j} \quad \text{in } K,$$

and, if we choose A_K^* constant in the definition (23), we obtain

$$\begin{cases} -\operatorname{div}\{A^\varepsilon \operatorname{grad} \Phi_i^{\varepsilon,K}\} \;=\; 0 & \text{in } K, \\ \\ \Phi_i^{\varepsilon,K} \;=\; p_i & \text{on } \partial K, \end{cases} \tag{28}$$

which is precisely the definition of the finite element basis in the multiscale method of Hou and Wu [13].

Remark 3.2. By changing the domain of definition of the local oscillating test functions $\widehat{w}_i^{\varepsilon,K}$ it is possible to devise an oversampling method in the spirit of [13], [11]. Instead of defining one such function for each cell K, we define a new local oscillating test function $\widehat{w}_i^{\varepsilon,l}$ for each node l of the coarse mesh. Let us denote by $\mathcal{K}_l$ the patch of cells K connected to the node l. Let Q_l be a domain which is larger than $\mathcal{K}_l$. We define $\widehat{w}_i^{\varepsilon,l}$ as the solution of (23) in the oversampled patch Q_l instead of K. Denoting by $w_i^{\varepsilon,l}$ its numerical approximation, we define a new finite element basis $\Phi_l^{\varepsilon,h}(x) = \Phi_l^h \circ w^{\varepsilon,l}(x)$. Although $w^{\varepsilon,l}$ is usually not equal to x on the boundary of $\mathcal{K}_l$, $\Phi_l^{\varepsilon,h}$ is still a conforming finite element basis because the support of Φ_l^h is $\mathcal{K}_l$. However, the support of $\Phi_l^{\varepsilon,h}$ may now be different from that of Φ_l^h, and its nodal values are also different.

4. Convergence proof in the periodic case. Although for its practical implementation our multiscale numerical method does not make any assumption on the possible type of heterogeneities or oscillations of the tensor A^ε, it is convenient to analyze its convergence in the context of periodically oscillating coefficients. In this section, we assume that $A^\varepsilon(x) = A(\frac{x}{\varepsilon})$, where $A(y)$ is a periodic, uniformly coercive, and bounded matrix in the unit cube $Y = (0,1)^n$. Our error analysis (Theorem 4.1) requires some smoothness of the tensor $A(y)$. On the one hand, we use a result of homogenization theory under the assumption that the solutions χ_i of the cell problem (4) belong to $W^{1,\infty}$. For this to hold, it is enough to assume that $A(y)$ is piecewise smooth, possibly discontinuous through smooth interfaces. On the other hand, we use a standard result in the numerical analysis of finite element methods for the local cell problems (23) (which defines the oscillating test functions). This last argument works for smooth coefficients, locally in each cell K, but is possibly discontinuous at the interface between two neighboring cells. Therefore, we shall assume that the tensor $A(y)$ is piecewise smooth, possibly discontinuous through smooth interfaces, and that

the mesh is aligned with the interfaces of discontinuity. Finally, we shall also need the homogenized solution u^* to be smooth. Since the homogenized tensor A^* is constant, this is easily obtained by assuming that the right-hand side f, as well as the domain Ω, are smooth enough.

Recall that we use a $\mathbb{P}_k$ Lagrange finite element method ($k \geq 1$) on the coarse mesh of size h and, locally on each cell K of the coarse mesh, a $\mathbb{P}_{k'}$ Lagrange finite element method on a fine mesh of size h' to compute the oscillating test functions. In order to use standard interpolation results for Lagrange finite elements we shall assume that the sequences of coarse meshes and fine meshes are quasi-uniform as h and h' tend to zero [9]. We always assume that

$$0 < h' < \varepsilon < h < 1.$$

THEOREM 4.1. *Let u^ε be the exact solution of (1) and $u_h^\varepsilon \equiv u_h \circ w^{\varepsilon,h}$ be the numerical solution of (25). Assume that $u^* \in W^{k+1,\infty}(\Omega)$ and $\chi_i \in W^{1,\infty}(Y)$. There exists a constant C independent of ε and h such that*

$$\|u^\varepsilon - u_h^\varepsilon\|_{H_0^1(\Omega)} \leq C \left(h^k + \sqrt{\frac{\varepsilon}{h}} + \left(\frac{h'}{\varepsilon}\right)^{k'} \right). \tag{29}$$

Remark 4.2. Using an oversampling method as explained in Remark 3.2 would improve slightly estimate (29) by replacing the $\sqrt{\varepsilon/h}$ term in its right-hand side (which is due to boundary layer effects) with ε/h. However, the resonance effect (i.e., the fact that the method does not converge if $h \approx \varepsilon$) does not disappear.

Proof. From Céa's lemma [9] applied to (25), there exists a constant C independent of ε and h such that

$$\|u^\varepsilon - u_h^\varepsilon\|_{H_0^1(\Omega)} \leq C \inf_{v_h^\varepsilon \in V_h^\varepsilon} \|u^\varepsilon - v_h^\varepsilon\|_{H_0^1(\Omega)}. \tag{30}$$

Define Π_h as the V_h-interpolation operator $\Pi_h\, v(x) = \sum_{l=1}^{N_h} v(n_l)\Phi_l^h(x)$, where n_l denotes the nodes associated with the $\mathbb{P}_k$ finite element method. We define an interpolation operator Π_h^ε, acting on V_h^ε: $\Pi_h^\varepsilon\, v(x) = \sum_{l=1}^{N_h} v(n_l)\Phi_l^{\varepsilon,h}(x)$. It satisfies $\Pi_h^\varepsilon\, v = (\Pi_h\, v) \circ w^{\varepsilon,h}$, but $\Pi_h^\varepsilon\, v(n_l) = v(n_l)$ only on those nodes n_l which belong to the element's boundaries ∂K. (This happens only for finite elements of order $k \geq 3$.)

In (30) we choose $v_h^\varepsilon = \Pi_h^\varepsilon u^*$, where u^* is the exact solution of the homogenized problem (5). This yields

$$\|u^\varepsilon - u_h^\varepsilon\|_{H_0^1(\Omega)} \leq C\, \|u^\varepsilon - \Pi_h^\varepsilon u^*\|_{H_0^1(\Omega)}. \tag{31}$$

Introducing the rescaled solution of the cell problem (4),

$$\widetilde{w}^\varepsilon(x) = x + \varepsilon \chi\left(\frac{x}{\varepsilon}\right), \tag{32}$$

we bound the right-hand side of (31):

$$\begin{aligned} \|\nabla u^\varepsilon - \nabla(\Pi_h^\varepsilon u^*)\|_{L^2(\Omega)^n} \leq\ & C \ \Big(\|\nabla u^\varepsilon - \nabla\,(u^* \circ \widetilde{w}^\varepsilon)\,\|_{L^2(\Omega)^n} \\ & + \|\nabla\{(\,u^* - \Pi_h u^*\,) \circ \widetilde{w}^\varepsilon\}\|_{L^2(\Omega)^n} \\ & + \|\nabla\{\Pi_h u^* \circ (\,\widetilde{w}^\varepsilon - \widehat{w}^{\varepsilon,h}\,)\}\|_{L^2(\Omega)^n} \\ & + \|\nabla\{\Pi_h u^* \circ (\,\widehat{w}^{\varepsilon,h} - w^{\varepsilon,h}\,)\}\|_{L^2(\Omega)^n}\ \Big). \end{aligned} \tag{33}$$

The upper bound (33), which gives the order of convergence of our multiscale finite element method, is made up of four terms. The first one is related to a corrector result in periodic homogenization. The second one is linked to an interpolation result for the coarse mesh $\mathbb{P}_k$ finite element method. The third one is related to an homogenization result for the local oscillating test functions. Finally, the fourth term is concerned with an error estimate for the $\mathbb{P}_{k'}$ finite element method used to compute the local oscillating test functions.

The first term in the right-hand side of (33) is bounded thanks to Lemma 2.14. The second term is bounded by

$$
\begin{aligned}
&\|[\nabla \widetilde{w}^\varepsilon]\{\nabla(u^* - \Pi_h u^*)\} \circ \widetilde{w}^\varepsilon\|_{L^2(\Omega)^n} \\
&\leq \|Id + [\nabla_y \chi]\|_{L^\infty(Y)} \|\{\nabla(u^* - \Pi_h u^*)\} \circ \widetilde{w}^\varepsilon\|_{L^2(\Omega)^n} \\
&\leq C\|Id + [\nabla_y \chi]\|_{L^\infty(Y)} \|\nabla(u^* - \Pi_h u^*)\|_{L^\infty(\Omega)^n} \\
&\leq C\, h^k \, \|Id + [\nabla_y \chi]\|_{L^\infty(Y)} \|u^*\|_{W^{k+1,\infty}(\Omega)}
\end{aligned}
\tag{34}
$$

by standard interpolation results for Lagrange $\mathbb{P}_k$ finite elements [9]. The third term in the right-hand side of (33) is

$$
\|[\nabla(\widetilde{w}^\varepsilon - \widehat{w}^{\varepsilon,h})]\{\nabla(\Pi_h u^*)\} \circ (\widetilde{w}^\varepsilon - \widehat{w}^{\varepsilon,h})\|_{L^2(\Omega)^n} \leq \|u^*\|_{W^{1,\infty}(\Omega)} \|\nabla(\widetilde{w}^\varepsilon - \widehat{w}^{\varepsilon,h})\|_{L^2(\Omega)^n}. \tag{35}
$$

To estimate the right-hand side of (35) we write

$$
\|\nabla(\widetilde{w}^\varepsilon - \widehat{w}^{\varepsilon,h})\|^2_{L^2(\Omega)^n} = \sum_{K \in \mathcal{T}_h} \|\nabla(\widetilde{w}^\varepsilon - \widehat{w}^{\varepsilon,h})\|^2_{L^2(K)^n},
$$

and we use Lemma 2.13 for each cell K: actually, $\widehat{w}^{\varepsilon,h}$ converges to x in $H^1(K)$ weakly as ε tends to 0 (for fixed h), so $\widetilde{w}^\varepsilon$ is exactly the sum of the homogenized limit and of the corrector term. Since K is of size h, its surface $|\partial K|$ is of order h^{n-1}, and the total number of cells K is of order h^{-n}. (Here we use again the quasi-uniformity of the coarse mesh.) Thus, we obtain

$$
\|\nabla(\widetilde{w}^\varepsilon - \widehat{w}^{\varepsilon,h})\|^2_{L^2(\Omega)^n} \leq C\frac{\varepsilon}{h}.
$$

Finally, the fourth term in the right-hand side of (33) is

$$
\begin{aligned}
&\|[\nabla(\widehat{w}^{\varepsilon,h} - w^{\varepsilon,h})]\{\nabla(\Pi_h u^*)\} \circ (\widehat{w}^{\varepsilon,h} - w^{\varepsilon,h})\|_{L^2(\Omega)^n} \\
&\leq \|u^*\|_{W^{1,\infty}(\Omega)} \|\nabla(\widehat{w}^{\varepsilon,h} - w^{\varepsilon,h})\|_{L^2(\Omega)^n}.
\end{aligned}
\tag{36}
$$

In the right-hand side of (36) we have the difference between an exact cell solution $\widehat{w}^{\varepsilon,h}$ and its numerical approximation $w^{\varepsilon,h}$. Now using the facts that the fine mesh is aligned with the interfaces of discontinuities of $A(y)$ and the oscillating test function $\widehat{w}^{\varepsilon,h}$ is piecewise smooth, and by standard interpolation results for Lagrange $\mathbb{P}_{k'}$ finite elements [9], we thus obtain

$$
\begin{aligned}
\|\nabla(\widehat{w}^{\varepsilon,h} - w^{\varepsilon,h})\|^2_{L^2(\Omega)^n} &= \sum_{K \in \mathcal{T}_h} \|\nabla(\widehat{w}^{\varepsilon,h} - w^{\varepsilon,h})\|^2_{L^2(K)^n} \\
&\leq C(h')^{2k'} \sum_{K \in \mathcal{T}_h} |\widehat{w}^{\varepsilon,h}|^2_{H^{k'+1}_{\text{piecewise}}(K)} \\
&\leq C(h')^{2k'} \sum_{K \in \mathcal{T}_h} \varepsilon^{-2k'} |K| \leq C(h'/\varepsilon)^{2k'}.
\end{aligned}
$$

Collecting all four terms, (33) yields

$$\|\nabla u^\varepsilon \ - \ \nabla(\Pi_h^\varepsilon u^*)\|_{L^2(\Omega)^n} \leq C\left(\sqrt{\varepsilon} + h^k + \sqrt{\frac{\varepsilon}{h}} + \left(\frac{h'}{\varepsilon}\right)^{k'}\right),$$

which implies (29). ∎

5. Numerical results. In this section, we experimentally study the convergence and accuracy of our multiscale method through numerical computations in the case of interest, i.e., $h \gg \varepsilon$. We consider both periodic and nonperiodic homogenization problems, the first one being useful for checking the accuracy of the method with the explicitly known asymptotic expansion of the solution and the second one showing the interest of this method for numerical homogenization.

5.1. Implementation details. Let us first outline some details of the implementation. For the sake of comparison we first implemented the method of Hou and Wu [13], based on the direct numerical computation of the base functions defined in (28). We checked (not shown here) that our multiscale method in the $\mathbb{P}_1$ case (denoted by $\mathbb{P}_1$-MSFEM), which is theoretically equivalent to the method of Hou and Wu, does indeed coincide numerically, although the implementations are quite different. The main novelty is the implementation of our $\mathbb{P}_2$ multiscale method (denoted by $\mathbb{P}_2$-MSFEM). As can be expected from the error estimate (29), its numerical results give a better approximation than the $\mathbb{P}_1$-MSFEM.

Once the coarse mesh of the domain Ω has been built with triangular elements, the implementation of the multiscale finite element methods is achieved in two steps.

The first step amounts to computing the elementary contributions (matrices and right-hand sides) from each cell of the coarse mesh for the boundary value problem at hand. It includes the computation of the oscillating functions $w^{\varepsilon,h}$, which can be done in parallel. To do so, each coarse element is meshed with triangles, and the oscillating functions $w^{\varepsilon,h}$ (which are numerical approximations of the solutions of the local problems (23) with A_K^* constant in K) are always computed with a $\mathbb{P}_1$ finite element method. The elementary stiffness matrices and the elementary right-hand side vectors are computed using numerical quadrature rules (two-dimensional centered trapezoidal rules).

After solving the oscillating functions, the stiffness matrix $[R^K]$ associated with $K \in \mathcal{T}_h$ is given by

$$\begin{aligned}[R^K] &= \int_K [\nabla\Phi^{\varepsilon,K}]^t A^\varepsilon [\nabla\Phi^{\varepsilon,K}]dx \\ &= \int_K [\nabla p^K]^t \circ w^{\varepsilon,K} [\nabla w^{\varepsilon,K}]^t A_\varepsilon [\nabla w^{\varepsilon,K}][\nabla p^K] \circ w^{\varepsilon,K} dx,\end{aligned} \tag{37}$$

where p^K stands for a polynomial basis function in $\mathbb{P}_k$ (see (26)). We can point out that, for the $\mathbb{P}_1$-MSFEM, the gradients of the base functions are constant and the composition rule with the oscillating functions does not play any role. For the $\mathbb{P}_2$-MSFEM, there is no such simplification, and the second line of (37) must be computed by using numerical quadrature rules. Introducing the local fine mesh $\mathcal{T}_{h'}^K$, the stiffness matrix is written

$$[R^K] = \sum_{T \in \mathcal{T}_{h'}^K} \int_T [\nabla\Phi^{\varepsilon,K}]^t A_\varepsilon [\nabla\Phi^{\varepsilon,K}]dx. \tag{38}$$

For smooth A^ε (as in section 5.2), a two-dimensional seven-point Gauss rule is used to compute the contributions of each element $T \in \mathcal{T}_{h'}^K$. Heterogeneous composite mediums which are described by piecewise constant properties (as in section 5.3) are treated in a different way. A weighted mean conductivity is computed which combines values of conductivity of the materials with the volumic fractions in the element $T \in \mathcal{T}_{h'}^K$. The elementary quantities are computed using a two-dimensional centered trapezoidal rule.

The next step of the implementation consists in assembling these elementary contributions to build the matrix and the right-hand side for the coarse mesh computation. Finally, after taking into account the boundary conditions on $\partial\Omega$, the resulting linear system is solved. In our implementation, all linear systems are solved by the Cholesky method.

5.2. Periodic setting. We first conduct numerical experiments in the periodic setting with a smooth scalar conductivity tensor (taken from [13]):

$$A^\varepsilon(x) \;=\; a(x/\varepsilon)\, Id,$$

where

$$a(x/\varepsilon) \;=\; 1/(2 + P\sin(2\pi x_1/\varepsilon))(2 + P\sin(2\pi x_2/\varepsilon)).$$

In this formula, P is used as a contrast parameter. ($P = 1.8$ for the numerical results presented here.) The right-hand side of the Dirichlet boundary value problem is $f = -1$. All computations are performed on the unit square domain Ω which is uniformly meshed by triangular finite elements (the coarse mesh of size h). Each triangle in this coarse mesh is again meshed by triangular finite elements (the local fine mesh of size $h' \ll h$). To make comparisons, we use another program. We compute, with a conjugate gradient method, a reference solution on a very fine mesh of 10^6 degrees of freedom, with a classical $\mathbb{P}_1$ finite element method (denoted by $\mathbb{P}_1$-FEM). We also compared our solution to the approximate one given by the first two terms of the two-scale asymptotic expansion. The homogenized conductivity is given by $A^* = 1/2(4 - P^2)^{1/2}$ (see [14]).

Comparison with the two-scale asymptotic expansion. A first obvious comparison is made between the two-scale asymptotic expansion (defined as the right-hand side of (2)) and the $\mathbb{P}_2$ multiscale finite element approximation for $\varepsilon = 10^{-2}$. This latter solution is computed on a coarse mesh with $h = 2 * 10^{-1}$ and a fine mesh $h' = 4 * 10^{-4}$. (This choice corresponds to $h' = h/500$.) The asymptotic expansion (denoted by $\mathbb{P}_1$-FEM AE) is built from $\mathbb{P}_1$ finite element approximations of the homogenized solution u^* and of the oscillating functions χ_i (see (2)). These latter ones are computed as solutions of (4) on the unit cell $Y = (0,1)^2$ with periodic boundary conditions. Figure 1 shows, as expected, a good approximation. The absolute errors are equal to $0.76\ 10^{-3}$ for the L^2-norm, $0.64\ 10^{-1}$ for the H^1-norm, and $0.25\ 10^{-2}$ for the L^∞-norm.

Resonance effects and optimal mesh scale. As we saw in the previous section, the theoretical bound of the *speed of convergence* of the method takes the form, for $k = 2$, $k' = 1$:

$$g^\varepsilon(h) \;=\; h^2 + \sqrt{\frac{\varepsilon}{h}} + \frac{h'}{\varepsilon}.$$

Although $g^\varepsilon(h)$ is only an upper bound of the true error, it indicates that there exists an optimal $h^*(\varepsilon)$ mesh size such that the numerical error, or at least g^ε, is minimum.

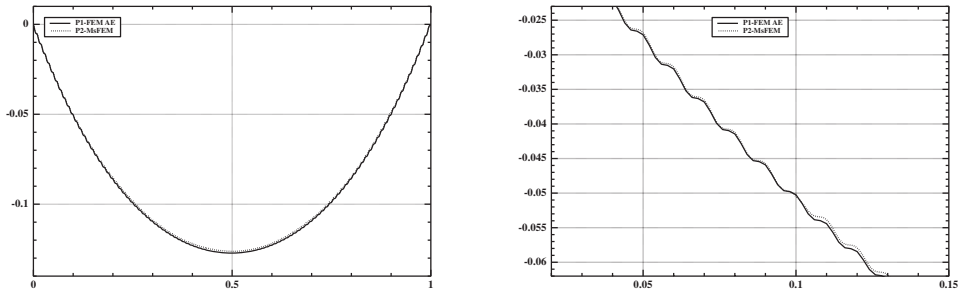

FIG. 1. *Cross sections at $y = 0.5$ of the rebuilt solution from asymptotic expansion and multiscale approximation (left) with a close-up (right): $\varepsilon = 10^{-2}$, $h = 1/5$, and $h' = 4.10^{-4}$.*

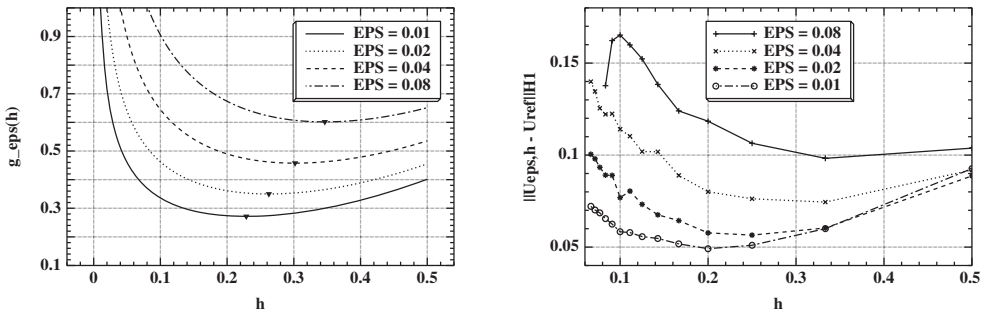

FIG. 2. *Error estimate predicted by formula* (39) *(left) and error estimate computed (right) as a function of h for different values of ε with $h' = 4.10^{-4}$.*

If we assume that h' is very small compared to ε, the order of this optimal value is

$$h^*(\varepsilon) \simeq \varepsilon^{1/5}. \tag{39}$$

According to [13] the resonance effect is the occurrence of large errors when the grid size h and the heterogeneity scale ε are close. This effect is also predicted by the above formula and is inherent to the multiscale framework used to compute the oscillating functions: the decomposition of the initial boundary value problems into independent smaller boundary value problems set on the coarse mesh element is somehow arbitrary.

The theoretical bound of the order of convergence, $g^\varepsilon(h)$, is not small when the discretization step h is close to ε (which is supposed to be very small). Therefore it is not a good idea to take h too small. Rather, in view of (39), the optimal discretization step $h^*(\varepsilon)$ is larger than ε. This is indeed confirmed by our numerical experiments shown on Figure 2, where one can see that the behavior of the true numerical error (right) is close to that of the upper bound $g^\varepsilon(h)$ (left). It clearly indicates that there exists an optimal mesh size h^* (larger than ε) which minimizes the numerical error. In the numerical experiments of Figure 2 we keep a constant value $h' = 4.10^{-4}$, but the same results hold true if we take instead $h' = h/M$ with a constant value $M = 500$. In Table 1, for $\varepsilon = 10^{-2}$, we give the computed error estimates as a function of h, not only in the H^1-norm but also in the L^2- and L^∞-norms. For these three norms the minimum is attained for the same value of $h = 0.2$. In Figure 2 and

TABLE 1

Error estimates (in various norms) as a function of h for $\varepsilon = 10^{-2}$ and $h' = 4.10^{-4}$ ($\mathbb{P}_2$-MSFEM).

h	$\| u_h^\varepsilon - u^\varepsilon \|_{L^2(\Omega)}$	$\| u_h^\varepsilon - u^\varepsilon \|_{H_0^1(\Omega)}$	$\| u_h^\varepsilon - u^\varepsilon \|_{L^\infty(\Omega)}$
0.0666	0.372 E-02	0.721 E-01	0.673 E-02
0.0769	0.327 E-02	0.685 E-01	0.792 E-01
0.0833	0.287 E-02	0.654 E-01	0.522 E-02
0.0909	0.264 E-02	0.624 E-01	0.513 E-02
0.1000	0.105 E-03	0.583 E-01	0.196 E-02
0.1250	0.146 E-02	0.557 E-01	0.273 E-02
0.1666	0.116 E-02	0.517 E-01	0.313 E-02
0.2000	0.412 E-03	0.491 E-01	0.243 E-02
0.2500	0.702 E-03	0.509 E-01	0.405 E-02
0.3333	0.195 E-02	0.600 E-01	0.604 E-02
0.5000	0.536 E-02	0.926 E-01	0.107 E-01

TABLE 2

Convergence toward the homogenized solution as a function of ε for the optimal $h^*(\varepsilon)$ and $h' = h^*(\varepsilon)/500$ ($\mathbb{P}_2$-MSFEM).

ε	$h^*(\varepsilon)$	$\| u_h^\varepsilon - u^* \|_{L^2(\Omega)}$	$\| u_h^\varepsilon - u^* \|_{L^\infty(\Omega)}$
0.01	0.20	0.150 E-02	0.332 E-02
0.02	0.20	0.246 E-02	0.510 E-02
0.04	0.33	0.594 E-02	0.139 E-01
0.08	0.33	0.408 E-02	0.921 E-02

Table 1 u^ε denotes the reference solution computed on a very fine (converged) mesh of 10^6 degrees of freedom with a classical $\mathbb{P}_1$ finite element method.

Convergence toward the homogenized solution. We fix the ratio $M = h/h'$ (equal to 500) large enough so that $h'/\varepsilon \ll 1$. Then, for different values of ε and for the optimal mesh size $h^*(\varepsilon)$, we compute the $\mathbb{P}_2$-MSFEM approximation u_h^ε. One can check on Table 2 that this numerical approximation clearly converges toward the homogenized solution u^* in the L^2- and L^∞-norms. We do not use the H^1-norm since, on the contrary of Figure 1, we do not add any corrector term to u^* (which is required for a good H^1-approximation, as is clear from (3)).

Comparison with a $\mathbb{P}_1$-MSFEM. We now make some detailed comparisons between the $\mathbb{P}_1$-MSFEM and $\mathbb{P}_2$-MSFEM in terms of the quality of the results and CPU time for $\varepsilon = 10^{-2}$ and $h' = h/500$ (with varying h). Let us first recall that our $\mathbb{P}_1$-MSFEM is identical to the method of Hou and Wu [13]. (Only the computer implementation is different.) For both the $\mathbb{P}_1$-MSFEM and the $\mathbb{P}_2$-MSFEM the main computational burden is the computation of the oscillating functions $w^{\varepsilon,h}$, which are exactly the same in both cases. The only difference between $\mathbb{P}_1$-MSFEM and $\mathbb{P}_2$-MSFEM stems from assembling the coarse mesh matrix and solving the associated linear system, which is of relatively small size. The cost of this coarse-scale computation is always negligible in front of the microscopic-scale computation of the oscillating functions $w^{\varepsilon,h}$ (even when the latter ones are computed in parallel; see Table 3). Therefore, there is almost no difference in the CPU costs of the $\mathbb{P}_1$-MSFEM and $\mathbb{P}_2$-MSFEM. In other words, it is always advantageous to use $\mathbb{P}_2$-MSFEM instead of $\mathbb{P}_1$-MSFEM since the former is more precise according to Table 4 (where u^ε denotes the reference solution computed on a fine mesh of 10^6 degrees of freedom with a classical $\mathbb{P}_1$ finite element method). Another conclusion that can be drawn from Table 3 is that our $\mathbb{P}_1$-MSFEM or $\mathbb{P}_2$-MSFEM is perfectly scalable in terms of

TABLE 3

*CPU times (in seconds) measured on a DELL Poweredge (with 2*3GHz P4 processors) with a total amount of memory of 40Go. N is the total number of elements in the coarse mesh. CPU1 is the total sequential time for computing the oscillating functions $w^{\varepsilon,h}$. (Thus CPU1/N is the corresponding parallel time.) CPU2 is the inherently sequential time for the coarse mesh computation (assembling and solving).*

$\varepsilon = 10^{-2}$		$\mathbb{P}_1$-MSFEM			$\mathbb{P}_2$-MSFEM		
h	N	CPU1 (s)	CPU2 (s)	CPU1/N (s)	CPU1 (s)	CPU2 (s)	CPU1/N (s)
0.0666	450	99188	1.05	220	81918	1.05	182
0.0769	338	72965	0.46	215	65508	0.46	193
0.0833	288	56299	0.30	195	57105	0.30	198
0.0909	242	46224	0.18	191	54620	0.18	225
0.1000	200	38478	0.11	192	47520	0.11	237
0.1250	128	26712	0.04	208	25640	0.04	200
0.1666	72	14388	0.02	199	14229	0.02	197
0.2000	50	11712	0.01	234	9897	0.01	197
0.2500	32	8234	0.01	257	6367	0.01	198
0.3333	18	4787	0.01	265	3619	0.01	201
0.5000	8	1847	0.00	230	1849	0.01	231

TABLE 4

Error estimates (in various norms) as a function of h for $\varepsilon = 10^{-2}$ and $h' = h/500$: $\mathbb{P}_1$-MSFEM (left), $\mathbb{P}_2$-MSFEM (right).

$\varepsilon = 10^{-2}$	$\mathbb{P}_1$-MSFEM		$\mathbb{P}_2$-MSFEM	
h	$\| u_h^\varepsilon - u^\varepsilon \|_{L^2(\Omega)}$	$\| u_h^\varepsilon - u^\varepsilon \|_{H_0^1(\Omega)}$	$\| u_h^\varepsilon - u^\varepsilon \|_{L^2(\Omega)}$	$\| u_h^\varepsilon - u^\varepsilon \|_{H_0^1(\Omega)}$
0.0666	0.442E-02	0.828E-01	0.346E-02	0.714E-01
0.0769	0.421E-02	0.834E-01	0.299E-02	0.670E-01
0.0833	0.398E-02	0.828E-01	0.260E-02	0.642E-01
0.0909	0.412E-02	0.837E-01	0.239E-02	0.610E-01
0.1000	0.289E-02	0.840E-01	0.955E-03	0.581E-01
0.1250	0.415E-02	0.921E-01	0.131E-02	0.547E-01
0.1666	0.581E-02	0.106E+00	0.107E-02	0.512E-01
0.2000	0.676E-02	0.117E+00	0.412E-03	0.491E-01
0.2500	0.929E-02	0.134E+00	0.702E-03	0.509E-01
0.3333	0.133E-01	0.154E+00	0.195E-02	0.600E-01
0.5000	0.155E-01	0.168E+00	0.536E-02	0.926E-01

moderate values of the total number N of elements in the coarse mesh. (Recall that the size of each microscopic problem is constant here, equal to $M = 500 = h/h'$.)

Effects of the boundary conditions for the oscillating functions. Imposing Dirichlet boundary conditions for the oscillating functions on each element K is a convenient, albeit arbitrary, choice. As a matter of fact it is one of the main problems of the method. Since the oscillating function $w^{\varepsilon,h}(x)$ is equal to the identity x on all boundary nodes on ∂K (see (23)), it cannot oscillate on these boundaries. Therefore our multiscale method cannot mimic the oscillating properties of the true solution locally on the boundaries of the coarse mesh cells K. This effect is easily seen when we consider cross sections of the solution along the sides of the elements of the coarse mesh (see Figure 3).

On the other hand, the oscillating behavior of the solution is well captured inside the coarse mesh elements where the oscillations of the oscillating function $w^{\varepsilon,h}(x)$ are fully developed. The cross sections of Figure 4 show a very good approximation of the solution.

Quite often in the literature, comparisons are made only on the value of the

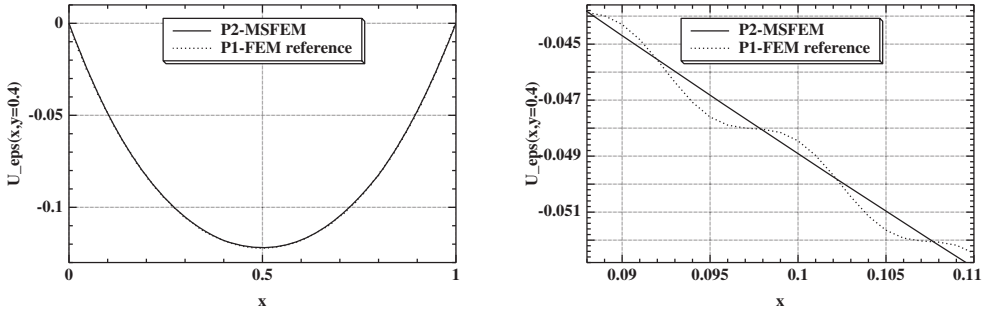

FIG. 3. *Cross sections along the side of the elements (left) and close-up (right) at* $y = 0.4$ *of the reference and multiscale solutions:* $\varepsilon = 10^{-2}$*,* $h = 1/5$*, and* $h' = 4.10^{-4}$*.*

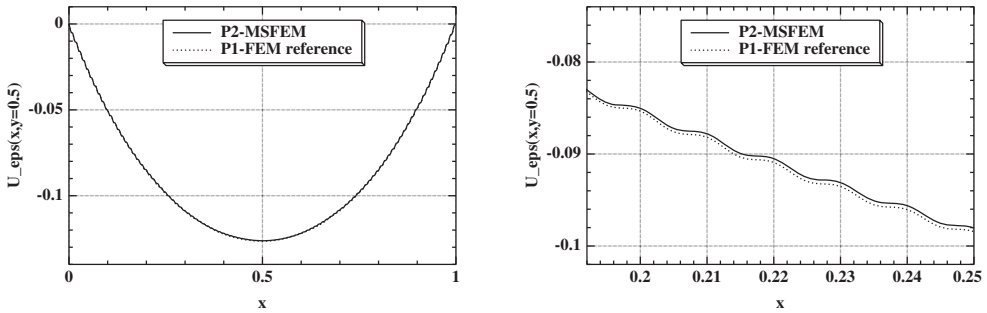

FIG. 4. *Cross section (left) and close-up (right) at* $y = 0.5$ *of the reference and multiscale solutions:* $\varepsilon = 10^{-2}$*,* $h = 1/5$*, and* $h' = 4.10^{-4}$*.*

unknown u^ε and not on the values of its partial derivatives. In the periodic setting, the asymptotic expansion (2) shows that this comparison is too naive and simple because the corrector term is of order ε, which is precisely small. On the other hand, the gradient asymptotic expansion (3) shows that the corrector term is of order 1 for the partial derivatives. Thus, a good comparison of the gradient implies that not only is the homogenized solution well captured, but so are the local fluctuations due to the corrector term. This is a well-known fact in homogenization theory, but it is maybe not so obvious in other fields. In any case, we believe it is very important, in the periodic setting at least, to make precise comparisons for the gradient $\mathrm{grad} u^\varepsilon$ or the flux $A^\varepsilon \mathrm{grad} u^\varepsilon$. This is done on Figures 5 and 6, where we see a remarkably good agreement, except at those nodes located at the coarse cell boundaries. As already explained, this last effect is due to the applied affine boundary conditions for the oscillating functions $w^{\varepsilon,h}$. Indeed, the overshoots and undershoots on Figures 5 and 6 take place precisely at the interface between two coarse mesh elements.

5.3. Two-phase composite material. Since the main interest of numerical homogenization is to compute approximate solutions in a nonperiodic setting, we consider a heterogeneous composite material made up of a pseudorandom distribution of spherical inclusions in a background matrix. In such a case, there is, of course, no reference solution or no explicit asymptotic expansion of the solution. As a model problem we consider the study of the conductivity properties (or antiplane elasticity properties) of a two-phase composite material made up of spherical inclusions in a background matrix. Both phases are isotropic with a high conductivity $A^\varepsilon(x) = 100$ in

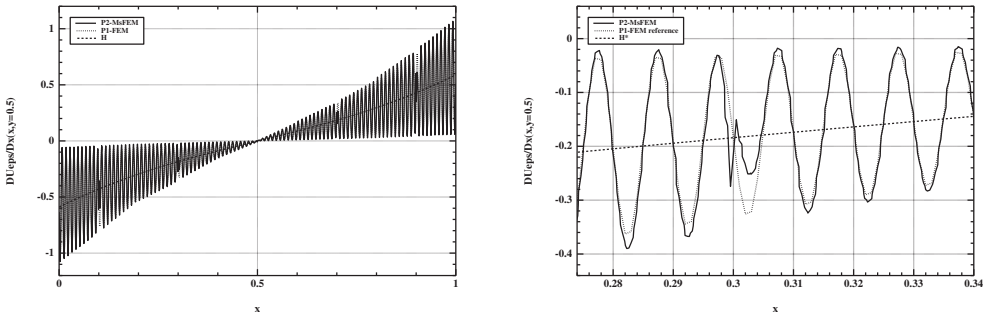

FIG. 5. *Cross section (left) and close-up (right) of the partial derivative* $\partial u^\varepsilon/\partial x$ *at* $y = 0.5$ *of the reference and multiscale solutions:* $\varepsilon = 10^{-2}$*,* $h = 1/5$*, and* $h' = 4.10^{-4}$*. Here* H *stands for the homogenized solution.*

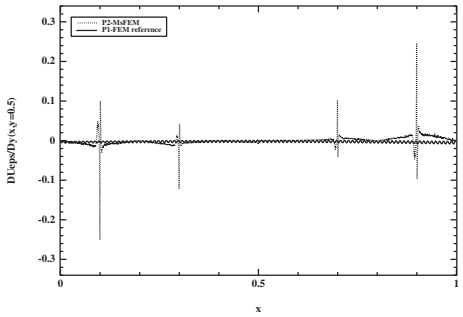

FIG. 6. *Cross section of the partial derivative* $\partial u^\varepsilon/\partial y$ *at* $y = 0.5$ *of the reference and multiscale solutions:* $\varepsilon = 10^{-2}$*,* $h = 1/5$*, and* $h' = 4.10^{-4}$*.*

the inclusions and a lower one $A^\varepsilon(x) = 1$ in the matrix. The inclusions are randomly distributed in the computational domain $\Omega = (0,1)^2$. On purpose we choose a large number of 10^6 inclusions so that a direct computation is out of reach with a standard finite element method. This numerical experiment corresponds to a minimum distance between two inclusions of $\varepsilon = 8{*}10^{-4}$ and a particle diameter of $\varepsilon/2$. We use a regular triangular coarse mesh with $h = 1/33$, and each coarse cell was supporting a local fine mesh which was also regular and triangular with $h' = h/500$. Figure 7 shows the coarse mesh and a close-up of the inclusions in one coarse cell.

We solve the elliptic equation (1) with zero right-hand side ($f = 0$) but with mixed nonhomogeneous boundary conditions:

(i) Dirichlet ones on the horizontal sides denoted by Γ_0 ($u_\varepsilon = 0$ on the lower side and $u^\varepsilon = 1$ on the upper one);

(ii) Neumann ones on the vertical sides denoted by Γ_1 ($A^\varepsilon \operatorname{grad} u^\varepsilon \cdot n = 0$, where n is the normal unit vector to $\partial\Omega$).

As already explained, the affine boundary conditions for the oscillating functions $w^{\varepsilon,h}$ break their necessary oscillating character on the coarse cell boundaries. This generates localized large errors for the gradient at those boundaries (see Figures 5 and 6). In the present case, since the conductivity jumps between the two phases, the errors are unacceptably large. Therefore, in order to circumvent this difficulty, we implemented another kind of boundary condition which gives a better approximation. Following an idea of [13] we solve one-dimensional elliptic problems on each line

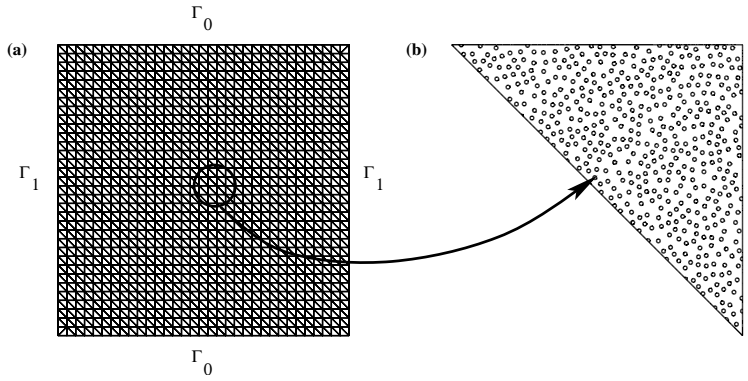

FIG. 7. (a) *the coarse mesh of* $\Omega = (0,1)^2$*;* (b) *close-up on the inclusions.*

segment of ∂K, and these one-dimensional solutions are used as boundary conditions for the oscillating functions $w^{\varepsilon,h}$. In other words, we change the boundary conditions in the local problems (23), and $w^{\varepsilon,h}$ is now defined as a numerical approximation in each coarse cell K of

$$\left\{ \begin{array}{rcll} -\mathrm{div}\{A^\varepsilon(x)\,\mathrm{grad}\,\widehat{w}_i^{\varepsilon,K}\} & = & 0 & \text{in } K, \\ \widehat{w}_i^{\varepsilon,K} & = & b_i^{\varepsilon,K}(x) & \text{on } \partial K, \end{array} \right. \tag{40}$$

where on each side S of the cell K, parametrized by a curvilinear coordinate $s \in [0,1]$, the boundary data $b_i^{\varepsilon,K}(x(s))$ is the solution of

$$-\frac{d}{ds}\left(A^\varepsilon(x(s))\frac{d\, b_i^{\varepsilon,K}}{ds} \right) = 0 \quad \text{for } x(s) \in S,$$

with the following boundary conditions at the two endpoints of S (which are corners of K):

$$b_i^{\varepsilon,K}(x(0)) = x_i(0), \quad b_i^{\varepsilon,K}(x(1)) = x_i(1),$$

which implies that the nodal values of $w^{\varepsilon,h}$ coincide with those of x. This modification of the boundary conditions for the oscillating functions $w^{\varepsilon,h}$ greatly improves the precision of the multiscale finite element method at the interface between two coarse mesh cells.

We do not display the approximated $\mathbb{P}_2$-MSFEM solution u^ε since, even at the scale of a single coarse cell, it varies almost linearly as the homogenized solution. As noticed before, a much more interesting numerical result is the profile of the flux field $A^\varepsilon \mathrm{grad}\, u^\varepsilon$, the norm of which is displayed on Figure 8. At a very small scale, one can clearly see the diffusion channels between close inclusions. This proves that our method is able to reproduce the fine details of the local fluctuations. Similarly on the right part of Figure 9 one can clearly see that the vertical derivative of u^ε has approximately an average value of 1 (which is compatible with the boundary conditions and the size of $\Omega = (0,1)^2$) and takes very small values when it crosses the highly conducting inclusions (which are almost perfect conductors with constant potential inside).

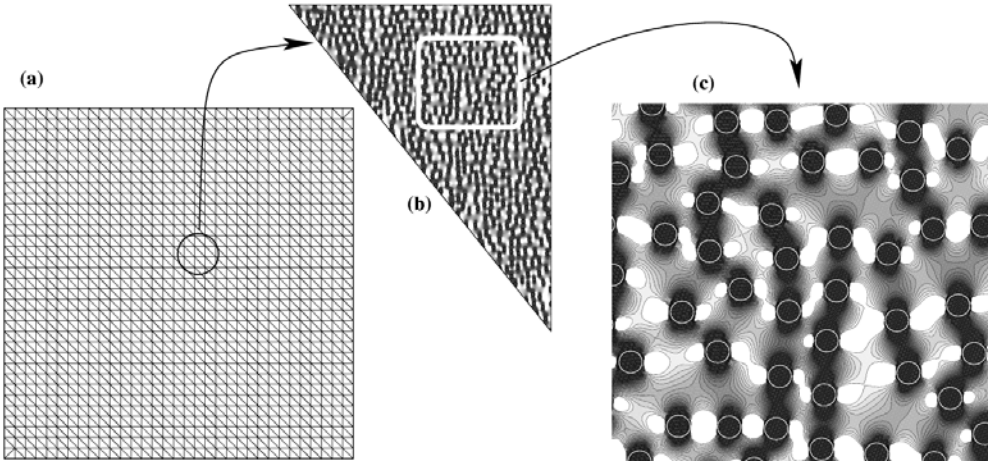

FIG. 8. (a) *the coarse mesh;* (b) *flux density, i.e.,* $\|A^\varepsilon \operatorname{grad} u^\varepsilon\|_{\mathbb{R}^2}$, *in an element of the coarse mesh; and* (c) *a close-up.*

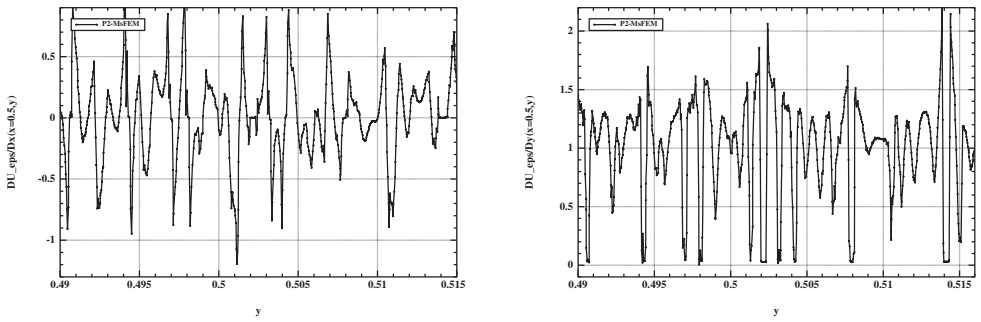

FIG. 9. *Close-up of the vertical cross sections of the partial derivatives* $\partial u^\varepsilon/\partial x(x = 0.5, y)$ *(left) and* $\partial u^\varepsilon/\partial y(x = 0.5, y)$ *(right) of the* $\mathbb{P}_2$*-MSFEM solution.*

REFERENCES

[1] G. ALESSANDRINI AND V. NESI, *Univalent σ-harmonic mappings*, Arch. Ration. Mech. Anal., 158 (2001), pp. 155–171.

[2] G. ALLAIRE, *Shape Optimization by the Homogenization Method*, Appl. Math. Sci. 146, Springer, New York, 2002.

[3] T. ARBOGAST, *Numerical subgrid upscaling of two-phase flow in porous media*, in Numerical Treatment of Multiphase Flows in Porous Media, Lecture Notes in Phys. 552, Z. Chen, R. E. Ewing, and Z. C. Shi, eds., Springer, Berlin, 2000, pp. 35–49.

[4] I. BABUŠKA, *Solution of interface problems by homogenization.* I, SIAM J. Math. Anal., 7 (1976), pp. 603–634.

[5] I. BABUŠKA, *Solution of interface problems by homogenization.* II, SIAM J. Math. Anal., 7 (1976), pp. 635–645.

[6] I. BABUŠKA, *Solution of interface problems by homogenization.* III, SIAM J. Math. Anal., 8 (1977), pp. 923–937.

[7] A. BENSOUSSAN, J. L. LIONS, AND G. PAPANICOLAOU, *Asymptotic Analysis for Periodic Structures*, Stud. Math. Appl. 5, North–Holland, Amsterdam, 1978.

[8] Y. CAPDEBOSCQ AND M. VOGELIUS, *Wavelet based homogenization of a* 2 *dimensional elliptic problem*, to appear.

[9] P. CIARLET, *The Finite Element Methods for Elliptic Problems*, North–Holland, Amsterdam, 1978.

[10] W. E. AND B. ENGQUIST, *The heterogeneous multiscale methods*, Commun. Math. Sci., 1 (2003), pp. 87–132.
[11] Y. R. EFENDIEV, T. Y. HOU, AND X.-H. WU, *Convergence of a nonconforming multiscale finite element method*, SIAM J. Numer. Anal., 37 (2000), pp. 888–910.
[12] Y. EFENDIEV AND X.-H. WU, *Multiscale finite element methods for problems with highly oscillatory coefficients*, Numer. Math., 90 (2002), pp. 459–486.
[13] T. Y. HOU AND X.-H. WU, *A multiscale finite element method for elliptic problems in composite materials and porous media*, J. Comput. Phys., 134 (1997), pp. 169–189.
[14] T. Y. HOU, X.-H. WU, AND Z. CAI, *Convergence of a multiscale finite element method for elliptic problems with rapidly oscillating coefficients*, Math. Comp., 68 (1999), pp. 913–943.
[15] S. M. KOZLOV, *Averaging of random operators*, Math. USSR-Sb., 37 (1980), pp. 167–180.
[16] A.-M. MATACHE, I. BABUSKA, AND C. SCHWAB, *Generalized p-FEM in homogenization*, Numer. Math., 86 (2000), pp. 319–375.
[17] A.-M. MATACHE AND C. SCHWAB, *Two-scale FEM for homogenization problems,* M2AN Math. Model. Numer. Anal., 36 (2002), pp. 537–572.
[18] N. G. MEYERS, *An L^p-estimate for the gradient of solutions of second-order elliptic divergence equations*, Ann. Scuola Norm. Sup. Pisa (3), 17 (1963), pp. 189–206.
[19] F. MURAT AND L. TARTAR, *H-convergence*, in Topics in the Mathematical Modeling of Composite Materials, Progr. Nonlinear Differential Equations Appl. 31, A. Cherkaev and R. V. Kohn, eds., Birkhaüser, Boston, 1997, pp. 21–43.
[20] P. H. RABINOWITZ, *Théorie du degré topologique et applications à des problèmes aux limites non linéaires*, rédigé par H. Berestycki, Laboratoire d'Analyse Numérique, Université de Paris VI, Paris, 1975.
[21] G. STAMPACCHIA, *Le problème de Dirichlet pour les équations elliptiques du second ordre à coefficients discontinus*, Ann. Inst. Fourier (Grenoble), 15 (1965), pp. 189–258.